University of BRISTOL

SCHOOL OF PHYSICS

FINAL YEAR PROJECT INTERIM REPORT

NAME:	Rory Tidmarsh
DEGREE COURSE:	Physics with Scientific Computing (Bsc)
PROJECT TITLE:	TP-B05 Wetting Robots
YEAR OF SUBMISSION:	2025
SUPERVISOR:	Dr. Francesco Turci
NUMBER OF WORDS:	*2561*

Simulating Emergent Behaviour in the Presence of a Repulsive Barrier Using the Vicsek Model

Rory Tidmarsh

January 16, 2025

Abstract

The well-known Vicsek model, which simulates the emergent behaviour of active particles using alignment interactions, is modified with a repulsive barrier to study the emergent motion near boundaries. Our model reveals that the particles flow in parallel with the barriers with increases in density occurring near the boundary due to conflicting alignment and repulsion interactions. For full length barrier systems, both parallel and antiparallel flows are observed, producing two sub-systems, whereas partial length systems produce a coherent system with parallel flow.

1 Introduction

Emergent or collective behaviour can be observed in nature at all sizes of living organisms, for example, bacteria colonies [1], schools of fish [2], herds of mammals [3] and swarms of locusts [4]. Simple rules between organisms at the individual level can lead to spontaneous emergent behaviour on a larger scale even without the need for a centralised leader, most dramatically demonstrated by starling murmurations [5]. This self-organisational behaviour creates decentralised systems that produce complicated motions and patterns that are not necessarily apparent from inspecting an individual, demonstrating the principle of "more is different" [6].

These self-organised systems are examples of active matter [7], a field of research focusing on self-propelled particles that continuously consume energy. While active particles can exhibit some equilibrium like behaviour in certain limits, their continuous energy consumption means the systems is evolves far from equilibrium. This non-equilibrium nature leads to phase transitions like the motility-induced phase separation (MIPS) [8] where particles slow down in denser particle population regions, causing an accumulation, which further increases the density. The generated positive feedback loop creates a separation between dense and less dense phases (analogous

to liquid-vapour phases), despite no attractive forces between particles.

Swarms of robots can simulate a decentralised system and investigate emergent behaviour. Autonomous robots can perform tasks without the need for a centralised control system. They can communicate and sense each other, to develop complex systems such as search and rescue operations [9], exploration tasks [10] and environmental monitoring [11]. Decentralised systems of robots allow for inexpensive, robust swarms of robots to go into harsh conditions with limited signal and perform tasks which would be hard for humans or centralised systems to complete. One minimalistic model of such robots are Kilobots [12], designed to be used in a swarm compromising hundreds or thousands of robots. Communication with each other occurs via IR detectors and sensors, performing simple rules leading to emergent behaviour of the Kilobot swarm.

Both robotic and biological systems exhibit interesting behaviour when interacting with boundaries. One way to model such systems is through active Brownian particles (ABPs), which combine the self-propulsion at a constant speed with randomness in the direction of motion, without any communication between particles [13]. When these active systems come into contact with a repulsive barrier, such as a wall or a solid object, then a wetting transition occurs which is similar to that seen in equilibrium systems of passive particles [14]. A wetting transition describes how a liquid interacts with a solid surface, resulting in two types of wetting effects. These are complete wetting, where the liquid phase spreads out across the surface, and partial wetting, where the liquid forms a droplet and the contact angle changes according to the surface tensions [15]. In the case of the active particles on a strong repulsive barrier then a complete wetting occurs [14]. Therefore a robot (Kilobot) set to walk in random directions (analogous to APBs) would get trapped (or wetted) to the wall, inhibiting the progress of any prescribed task.

To understand the interactions in these active matter systems several simplistic models have been developed. The Vicsek model [16] was created to mimic the motion of biological systems like flocks of birds, it simplifies the behaviour of the motion of the active particles by keeping a constant particle speed and only altering their direction of movement. This creates a minimalistic model with little microscopic detail but retains the properties of the system's long-term behaviour [17].

While the Vicsek model effectively describes the motion of active systems, it was originally developed without constraints. By introducing a verticle repuslive barrier into the Vicsek model, this study aims to understand how collective behaviour in both robotic and biological systems with obstacles. These ideas can be developed into evolving algorithms in robotics to stop the collection of robots at boundaries.

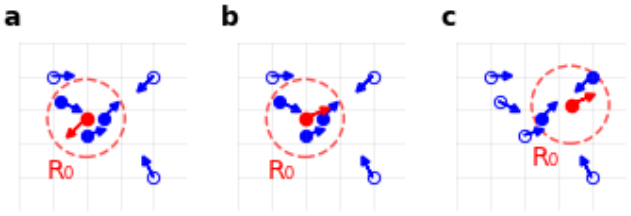

Figure 1: Cartoon representation of the angle calculation for the Vicsek model. The particle in red aligns with the particles inside a given radius, R_0, that are shown in dark blue. a) shows an initial condition, b) the angle alignment for the red particle and c) the position at the next time step before reorientating. This only shows the update for the red particle but in the complete algorithm, all the particles update simultaneously.

2 Theory

There are several existing theoretical models for simulating active particle behaviour, each tailored to different aspects of emergent group motion. The active Brownian particle (ABP) model [13] describes the motion of particles at a constant speed but continuously occurring random changes in direction. In the Run and Tumble model [18] particles alternate between straight runs of constant velocity and a sharp, randomised change in direction. The Toner-Tu [19] model describes the system using continuous dynamical equations using the density and velocity fields. Both the ABP and Run and Tumble models are simplistic forms of representing the motion of the particles on the individual level, but lack any interactions between particles. The Toner-Tu represents the system on a large scale and is mathematically complex, meaning it is less suitable for implementing barrier boundary conditions or translating to robotic systems.

2.1 Vicsek Logic

The Vicsek model maintains simplicity by having constant velocity and only variation in orientation. Orientation is updated due to an alignment interaction between particles, where a particle will reorientate itself to the average direction of other local particles. This creates emergent behaviour on the macroscopic scale of the system whilst maintaining mathematical simplicity. The simplicity allows for translation into computer simulation and modification to include interactions with boundaries to investigate wetting and allows ideas to be passed onto other more complicated systems.

The particle motion is described by the following key equations. The position of the particle is updated for the each iteration using

$$\vec{x_i}(t + \Delta t) = \vec{x}_i(t) + \vec{v_i}(t)\Delta t, \tag{1}$$

where Δt is the time between steps, $\vec{v_i} = v_0\hat{s_i}$ and $\hat{s_i}$ is the unit vector giving the orientation of particle i and v_0 is the constant speed of all particles. The orientation defined by

$$\hat{s_i} = \cos(\theta_i)\hat{x} + \sin(\theta_i)\hat{y}, \tag{2}$$

where θ_i is the angle to the x-axis. The angle θ_i is defined by

$$\theta_i(t + \Delta t) = \langle\theta(t)\rangle_{R_0} + \Delta\theta, \tag{3}$$

where $\langle\theta(t)\rangle_{R_0}$ is the average angle of all other particles within a given radius, R_0, as can be seen in Figure 1. $\Delta\theta$ represents the noise in the system and for any given particle and time is given a randomised value from a uniform distribution in the interval $[-\eta/2, \eta/2]$, η numerically describing the noise in the system. Figure 1 gives a visualisation of how these equations evolve.

Equations 1-3 are applied to all the particles in the system at each step and the positions are all updated simultaneously. The Viscek model is initialised by randomising the particle positions and orientations and applying periodic boundary conditions. Three key parameters control the behaviour of the system: particle density ρ, interaction radius R_0 and noise η. At small densities and noise particles collect into small groups that move coherently and in random directions [16]. Increasing the noise leads to the particles moving with increasing disorder, however, containing some localised similarities in direction. With large densities and low noises, the system becomes ordered with all particles orientated in the same direction.

2.2 Boundary Logic

In order to implement the boundary conditions on a vertical wall the orientation calculation required modification. When the particle approaches the wall, within a certain distance r_w, then it receives a repulsive artificial force, f_i, away from the wall. This force scales inversely with the distance away from the wall, $\vec{r}$, and can be calculated by

$$\vec{f_i}(\vec{r}) = \frac{\alpha}{|r|}\hat{r} \qquad |r| \leq r_w, \tag{4}$$

where α is a constant that determines how strong the repulsion is. If the particle is within the limits of the wall $[y_{min}, y_{max}]$, then $\hat{r} = \pm\hat{x}$, else if it is above the top or below the bottom wall there is also a component in the $\hat{y}$ direction. The new particle velocity of the particle is given by $\vec{v_i} = v_0\hat{s_i^w}$, where $\hat{s_i^w}$ is the particle direction when is being repelled by the wall, given by

$$\vec{s_i^w} = \hat{s_i} + \vec{f_i}, \tag{5}$$

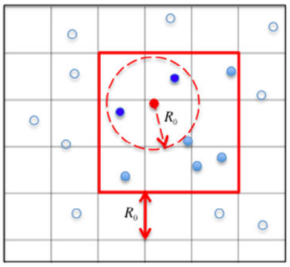

Figure 2: Taken from Ginneli [17]. Computational grid search to find neighbouring particles. This searching technique means the algorithm does not have to look at all particles to calculate the distance from them, just the ones in adjacent sections in the grid, increasing its efficiency.

where $\hat{s_i}$ is the reorientation due to the neighbours as stated in Equation 2. This creates a repulsive force for particles near the wall but is still affected by the alignment of neighbouring particles. The inverse proportionality between particle reorientaion, f_i and the distance from the wall r means as a particle gets closer to the wall the direction of travel is more increasingly affected by the wall repulsion. This type of inverse proportionality to the distance was designed to mimic how birds detect and then turn away from a wall to avoid collisions with a more drastic turn closer to the wall.

3 Computational Implementation

Starting from an in-house Python code, a simulation for the Vicsek model with a wall was developed, with various techniques used to optimise and improve the efficiency of the code. When calculating the average angle and the repulsion from the wall, the angles were expressed as complex exponentials, with the real and imaginary axis representing the x and y axes respectively. This meant the complex number representing the direction of the i^{th} particle for j particles within the radius R_0 is

$$z_i = \frac{\alpha}{|z_{wall}|}z_{wall} + \sum_j z_j \qquad z \in \mathbb{C}. \tag{6}$$

This ensured a fair balance between the repulsion from the wall and the alignment factor from nearby particles. The angle was calculated by taking the argument of z.

A straightforward approach to calculate the alignment component was the comparison of $i-j$ particles, creating a N^2 scaling for the system. This quickly reduced the simulation speed as the number of particles, N, increased. To mitigate this, the system was sub-divided into a grid containing small squares with side-length R_0 and for each time-step each particle was assigned to a square in the

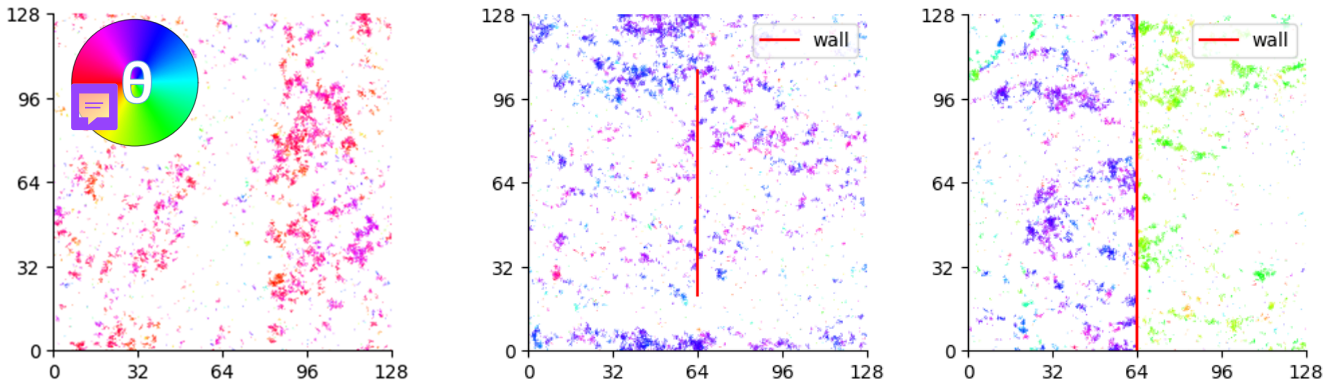

(a) No wall. (b) Wall length, $l = \frac{2}{3}L$. (c) Wall length, $l = 1L$.

Figure 3: Example positions of the Vicsek model in the steady state of their various sized walls.

grid. To search for the particles within the radius, R_0 the algorithm only had to look in the box containing particle i and the neighbouring boxes. This reduced the search area per particle to 9 boxes in 2 dimensions, see Figure 2 for a visualisation.

The next optimisation of the program used Numba [20] to speed up the code runtime. Numba is a just-in-time (JIT) compiler that translates CPython code, compromising of lots of NumPy ndarrays and numeric scalars, into machine readable code that is similar speeds to compiled language code. Important functions including neighbour searching, wall interaction and angle calculation were accelerated using Numba's parallelisation decorators.

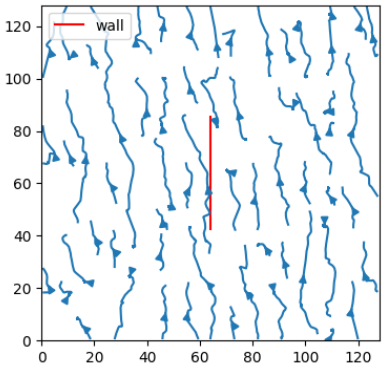

Figure 4: Stream plot representing the flow of particles in the steady state for $l = \frac{1}{3}L$.

4 Results

The addition of the repulsive barrier to the Vicsek model alters the collective motion of the particles. For the simulations discussed the verticle wall was implemented halfway across a square grid, with side lengths $L = 128$. Distances are measured in arbitrary spatial units with the interaction radius $R_0 = 0.65A.U.$, giving $L = 197R_0$. The density and noise were chosen to be $\rho = 1$, $\eta = 0.1$, as that produced a system with particles moving in the same direction but also produced clusters, see Figure 3a. Here the bands described in [17] are faintly produced, as can be seen by a low-density region followed by a higher-density region at $x = 80A.U.$ in Figure 3a.

When the barrier is implemented the movement of the particles in the steady state changes from flowing in a random direction to a flowing up or down the barrier. This behaviour can clearly be seen in the stream plot in Figure 4, where the stream lines run approximately parallel to the barrier (with slight variation due to the noise η). The average orientation of the particles, $\langle\theta\rangle$ can be defined as the argument of the sum of the complex orientation of all the particles,

$$\langle\theta\rangle = \arg(\sum_i z_i), \tag{7}$$

which converges to approximately $\langle\theta\rangle \approx \pm\frac{\pi}{2}$, confirming the parallel motion to the wall (Figure 5a). However, for the wall length $l = 1L$, the system does not always appear to align up or down the wall, as demonstrated by the large fluctuations in orientation in Figure 5a. This system can produce two distinct regions with anti-parallel flows, visible in Figure 3c. This also explains the larger spread of angle, $\sigma(\theta)$, for $l = 1L$ in Figure 5b.

The spread of particle orientations can provide further insight into the time evolution of the system. For the wall length $l < L$, the system has a large standard deviation $\sigma(\theta)$, in the initial transient phase (see Figure 5b). Once the system reaches a steady state ($t > 3000 - 5000$, varying due to initial conditions), this is reduced to $\sigma(\theta) \approx 0.5$. However, for $l = L$ the variation can settle down to $\sigma(\theta) = 0.5$ for parallel steady states or

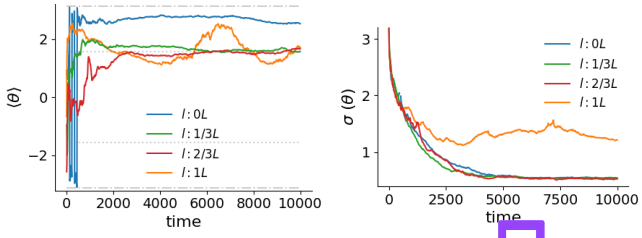

(a) Average orientation $\langle\theta\rangle$ (b) Spread of angles $\sigma(\theta)$

Figure 5: Average orientation of angles converging to $\langle\theta\rangle \approx \pm\pi/2$ for wall heights $0 < l < 1L$ and spread of angles converging to $\sigma(\theta) \approx 0.5$ for the original Vicsek model and for wall lengths $l < 1L$. The spread of angles (b) is averaged from 6 simulations, whereas (a) is from 1 simulation.

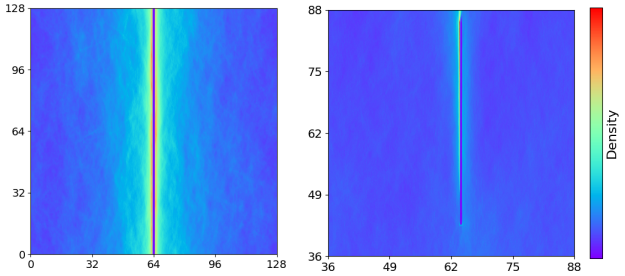

(a) Full size wall, $l = L$. (b) $l = \frac{1}{3}L$ wall.

Figure 6: Spatial distribution of particles in the steady state, averaged over 6 simulations with the red regions signifying highest density. 6b is zoomed in close to the wall to clarify density increase around the wall. Particles accumulate at approximately $|\Delta x| \approx 1.5$ away from the infinitely thin wall where $\alpha = 0.2$.

have a continuously large spread for the antiparallel case.

Once the system has reached the steady state, the spatial distribution of particles was calculated by creating 2D density histograms, Figure 6. The density histogram shows higher particle concentrations near the barrier compared to the rest of the system. This accumulation is consistent with all walls, but is more prominent for $l = 1L$.

5 Discussion

The wetting behaviour observed with the Vicsek model differs vastly from that described with Active Brownian Particles (ABPs). While the ABPs gather near boundaries due to physical interactions and continuous motion [13], the Vicsek model demonstrates the alignment interactions between particles. The accumulation near the wall, Figure 6, occurs alongside the flow patterns running parallel to the barrier, Figure 4. This suggests that rather than the particles being trapped near the walls, as demonstrated for ABPs [14], then the particles flow along the boundary with continuous motion.

Higher particle density regions near the barrier, Figure 6, originate from the balance of interactions between particle alignment and the interaction of the wall. As a particle in a group approaches the wall the group alignment will try to maintain the orientation of particle into the barrier while the repulsive force pushes the particle away. The transition between the alignment interaction at a fixed distance, R_0, and the radial reduction in force creates a characteristic distance where the particles flow a distance $\Delta x \approx 1$ away from the wall.

The emergence of antiparallel flows for wall length $l = L$ appears due to the complete divide the barrier produces. In a system where $l < L$ then the particles have space to interact and align after travelling down the length of the wall. The absence of this space means the particles on either side of the barrier no longer interact, effectively creating two sub-systems on opposing sides of the barrier. These two sub-systems are either parallel or antiparallel, with the emergence of which coming from the evolution of the randomised states and the noise, η.

Using the Vicsek model in modelling the collective motion of a system with a barrier comes with some limitations. The simplified inverse relationship between the repulsive force and the distance, described in Equation 4, mimics biological sensing but may not be accurate for representing more complicated systems such as robotic systems where the sensors produce different responses.

The instantaneous nature of the Vicsek model must be considered too. In other systems, particularly in robotics, interactions occur with response delays, potentially causing a higher particle density near the wall since the particles take longer to communicate about the presence of a barrier. Other effects like the constant velocity, no hard particle interactions, periodic boundary conditions at the edge of the square system and uniform noise implementation must also be considered when developing this system.

6 Conclusion

The Vicsek model with a repulsive barrier demonstrates a collective behaviour different from that of Active Brownian Particles. Particles form dynamic flows along the boundary rather than a static accumulation that produces complete wetting. The emergence of flow parallel to the boundary and density accumulation near the boundary arise from the conflicting alignment and wall repulsion interactions. For full-length barrier systems, the system can evolve into parallel or antiparallel states, creating what is almost two subsystems. Further inves-

tigation into this model could explore how varying noise affects the flow states and the accumulation at the boundary.

Our future work will explore translating the alignment-based interactions into algorithms in the Kilombo simulator [21] for Kilobots. This addresses the challenge of Kilobots collecting at boundaries by implementing neighbour detection and alignment interactions. More complexity is added to the system when real-world constraints like response delays and sensors' limitations are applied. This future step will need to consider the capabilities that the Kilobots have to apply and adapt the insights from the Vicsek model into swarm robotics.

References

[1] H. P. Zhang et al., "Collective motion and density fluctuations in bacterial colonies", Proceedings of the National Academy of Sciences **107**, _eprint: https://www.pnas.org/doi/pdf/10.1073/pnas.1001651107, 13626–13630 (2010) 10.1073/pnas.1001651107.

[2] Y. Katz et al., "Inferring the structure and dynamics of interactions in schooling fish", Proceedings of the National Academy of Sciences **108**, Publisher: Proceedings of the National Academy of Sciences, 18720–18725 (2011) 10.1073/pnas.1107583108.

[3] F. Ginelli et al., "Intermittent collective dynamics emerge from conflicting imperatives in sheep herds", Proceedings of the National Academy of Sciences **112**, _eprint: https://www.pnas.org/doi/pdf/10.1073/pnas.1503749112, 12729–12734 (2015) 10.1073/pnas.1503749112.

[4] G. Ariel and A. Ayali, "Locust Collective Motion and Its Modeling", en, PLOS Computational Biology **11**, Publisher: Public Library of Science, e1004522 (2015) 10.1371/journal.pcbi.1004522.

[5] A. E. Goodenough et al., "Birds of a feather flock together: Insights into starling murmuration behaviour revealed using citizen science", en, PLOS ONE **12**, Publisher: Public Library of Science, e0179277 (2017) 10.1371/journal.pone.0179277.

[6] P. W. Anderson, "More Is Different", Science **177**, Publisher: American Association for the Advancement of Science, 393–396 (1972) 10.1126/science.177.4047.393.

[7] G. Gompper et al., "The 2020 motile active matter roadmap", en, Journal of Physics: Condensed Matter **32**, Publisher: IOP Publishing, 193001 (2020) 10.1088/1361-648X/ab6348.

[8] M. E. Cates and J. Tailleur, "Motility-Induced Phase Separation", en, Annual Review of Condensed Matter Physics **6**, Publisher: Annual Reviews, 219–244 (2015) 10.1146/annurev-conmatphys-031214-014710.

[9] J. Jennings, G. Whelan, and W. Evans, "Cooperative search and rescue with a team of mobile robots", in 1997 8th International Conference on Advanced Robotics. Proceedings. ICAR'97 (July 1997), pp. 193–200, 10.1109/ICAR.1997.620182.

[10] A. Batinović et al., "Decentralized Strategy for Cooperative Multi-Robot Exploration and Mapping", IFAC-PapersOnLine, 21st IFAC World Congress **53**, 9682–9687 (2020) 10.1016/j.ifacol.2020.12.2618.

[11] M. Duarte et al., "Application of swarm robotics systems to marine environmental monitoring", in OCEANS 2016 - Shanghai (Apr. 2016), pp. 1–8, 10.1109/OCEANSAP.2016.7485429.

[12] M. Rubenstein, C. Ahler, and R. Nagpal, "Kilobot: A low cost scalable robot system for collective behaviors", in 2012 IEEE International Conference on Robotics and Automation, ISSN: 1050-4729 (May 2012), pp. 3293–3298, 10.1109/ICRA.2012.6224638.

[13] P. Romanczuk et al., "Active Brownian particles", en, The European Physical Journal Special Topics **202**, 1–162 (2012) 10.1140/epjst/e2012-01529-y.

[14] F. Turci, R. L. Jack, and N. B. Wilding, "Partial and complete wetting of droplets of active Brownian particles", en, Soft Matter **20**, Publisher: The Royal Society of Chemistry, 2060–2074 (2024) 10.1039/D3SM01493B.

[15] D. Bonn et al., "Wetting and spreading", Reviews of Modern Physics **81**, Publisher: American Physical Society, 739–805 (2009) 10.1103/RevModPhys.81.739.

[16] T. Vicsek et al., "Novel Type of Phase Transition in a System of Self-Driven Particles", en, Physical Review Letters **75**, 1226–1229 (1995) 10.1103/PhysRevLett.75.1226.

[17] F. Ginelli, "The Physics of the Vicsek model", en, The European Physical Journal Special Topics **225**, 2099–2117 (2016) 10.1140/epjst/e2016-60066-8.

[18] K. Martens et al., "Probability distributions for the run-and-tumble bacterial dynamics: An analogy to the Lorentz model", en, The European Physical Journal E **35**, 84 (2012) 10.1140/epje/i2012-12084-y.

[19] J. Toner and Y. Tu, "Long-Range Order in a Two-Dimensional Dynamical XY Model: How Birds Fly Together", en, Physical Review Letters **75**, 4326–4329 (1995) 10.1103/PhysRevLett.75.4326.

[20] S. K. Lam, A. Pitrou, and S. Seibert, "Numba: a LLVM-based Python JIT compiler", in Proceedings of the Second Workshop on the LLVM Compiler Infrastructure in HPC, LLVM '15 (Nov. 2015), pp. 1–6, 10.1145/2833157.2833162.

[21] F. Jansson et al., *Kilombo: a Kilobot simulator to enable effective research in swarm robotics*, arXiv:1511.04285 [cs], May 2016, 10.48550/arXiv.1511.04285.